

Cupiennius salei: biomechanical properties of the tibia–metatarsus joint and its flexing muscles

Tobias Siebert · Tom Weihmann · Christian Rode · Reinhard Blickhan

Received: 11 March 2009 / Revised: 20 July 2009 / Accepted: 17 August 2009 / Published online: 16 September 2009
© Springer-Verlag 2009

Abstract Hunting spiders are well adapted to fast locomotion. Space saving hydraulic leg extension enables leg segments, which consist almost solely of flexor muscles. As a result, the muscle cross sectional area is high despite slender legs. Considering these morphological features in context with the spider's segmented C-shaped legs, these specifics might influence the spider's muscle properties. Moreover, these properties have to be known for modeling of spider locomotion. *Cupiennius salei* ($n = 5$) were fixed in a metal frame allowing exclusive flexion of the tibia–metatarsus joint of the second leg (counted from anterior). Its flexing muscles were stimulated supramaximally using needle electrodes. Accounting for the joint geometry, the force–length and the force–velocity relationships were determined. The spider muscles produce 0.07 N cm maximum isometric moment (corresponding to 25 N/cm² maximum stress) at 160° tibia–metatarsus joint angle. When overextended to the dorsal limit at approximately 200°, the maximum isometric moments decrease to 72%, and, when flexed to the ventral hinge stop at 85°, they drop to 11%. The force–velocity relation shows the typical hyperbolic shape. The mean maximum shortening velocity is 5.7 optimum muscle lengths per second and the mean curvature (a/F_{iso}) of the Hill-function is 0.34. The spider muscle's properties which were determined are similar to those of other species acting as motors during locomotion (working range, curvature of Hill hyperbola, peak power at the preferred speeds), but they are relatively slow. In

conjunction with the low mechanical advantage (muscle lever/load arm), the arrangement of three considerably actuated joints in series may nonetheless enable high locomotion velocities.

Keywords Spider · Muscle properties · Force–velocity · Force–length · Contraction dynamics · Arthropod

Introduction

As a taxonomic category, spiders are rather old and their anatomy, on the whole, has not changed for hundreds of millions of years. Nonetheless, ecologically, they are still extraordinarily successful. Ethologically, they can be subdivided roughly into web spiders and hunting spiders. Hunting spiders are well adapted to locomotion. Specific features of all spiders are the slender C (bow)-shaped legs, which consist almost solely of flexor muscles (Blickhan and Barth 1985). In contrast to all other arthropods and even to most taxa within the chelicerata, the major leg joints (femur–patella joint, tibia–metatarsus joint) of spiders are characterized by a dorsal pivot and do not contain extensor muscles (Ellis 1944; Dillon 1952; Whitehead and Rempel 1959; Clarke 1986). Deviating from the typical antagonistic muscle design, these hinge joints are extended by hydraulic pressure generated in the prosoma (Parry and Brown 1959; Stewart and Martin 1974; Anderson and Prestwich 1975). Therefore, during locomotion, the flexor muscles must counteract extension forces resulting from increased internal pressure (Stewart and Martin 1974). These spider specifics probably not only characterize their global motion strategies (Parry and Brown 1959; Weihmann and Blickhan 2006; Moya-Larano et al. 2008) but also influence their muscle properties.

Communicated by G. Heldmaier.

T. Siebert (✉) · T. Weihmann · C. Rode · R. Blickhan
Institute of Motion Science, Friedrich Schiller University,
Seidelstraße 20, 07749 Jena, Germany
e-mail: tobias.siebert@uni-jena.de

The flexor muscles of the spider's legs are involved in all kinds of idiomotion and locomotion, for example catching prey, climbing, jumping and running (Ehlers 1939; Melchers 1967; Blickhan and Barth 1985; Weihmann and Blickhan 2006). Therefore, knowledge of their muscle properties is the precondition for the researcher to better understand movement generation (Siebert et al. 2007) and control mechanisms (Blickhan et al. 2003, 2007). Moreover, such knowledge may enable realistic simulation of spider movement.

The two most important muscle properties are the force–velocity relation (Hill 1938) resulting from the cross-bridge cycle, and the force–length relation, which is related to the actin–myosin overlap (Gordon et al. 1966). Only a few studies have dealt with dynamic leg muscle properties of walking arthropods. For example, several leg extensors in cockroaches (Ahn and Full 2002; Ahn et al. 2006) and a leg extensor in stick insects (Guschlbauer et al. 2007) have been examined. However, to date, dynamic spider leg muscle properties have not been studied.

In musculoskeletal systems, activated muscles produce joint movement and moments. Using morphometric data and geometric functions, it is possible to calculate muscle length and force from measured external force and length change (Leedham and Dowling 1995; Wagner et al. 2005; Siebert et al. 2007).

During the stance phase, the second legs of *Cupiennius salei* support level locomotion by flexing the semi-hydraulic leg joints (Blickhan et al. 2005). When the hydraulically extended femur–patella joint with four monoarticular and four biarticular muscles (Ruhland and Rathmayer 1978) is compared to the tibia–metatarsus hinge joint, we find that the latter is more accessible and its three flexing monoarticular muscles can conveniently be replaced by one artificial muscle. In this study, we focus on the biomechanical properties of the tibia–metatarsus joint and its flexing muscles.

The aims of the study were (1) to determine the force–length and the force–velocity relation of the tibia–metatarsus joint flexors, and (2) to compare these muscle properties with other arthropod muscles. Therefore, we investigated active and passive moment–angle and moment–angular velocity relations of the tibia–metatarsus joint as well as the geometric joint characteristics. These data were used to derive the force–length relationship and the force–velocity relationship of the metatarsus flexors substituted by one replacement muscle.

Materials and methods

Experiments were carried out on five female specimens of the typical hunting spider *Cupiennius salei* (S1–S5)

common in Central America. We examined the second leg (counted from anterior) with a metatarsus length $L_{\text{met}} = 13.0 \pm 1.0$ mm. All experiments were performed under daylight conditions at room temperature (20–22°C).

Three monoarticular muscles flex the tibia–metatarsus joint. The *M. flexor metatarsis longus* (FML) accounts for about 60% of physiological cross sectional area (CSA), whereas *M. flexor metatarsis accessorius* (FMA) and *M. flexor metatarsis bilobatus* (FMB) capture about 20% CSA each (Blickhan and Barth 1985). The FML originates from the proximal rim of the tibia, and the FMA and FMB originate from the dorsal surface of the tibia (Blickhan and Barth 1985). FML and FMA insert via an apodeme and an articulate joint membrane on the ventral rim of the proximal metatarsus border. FMB inserts directly on the proximal metatarsus border and has nearly half the muscular lever arm with respect to the tibia–metatarsus joint compared to FML and FMA. For simplicity, all muscles were described by one artificial substitute, which is termed muscle throughout the manuscript.

Preparation

Spiders were anesthetized with CO₂ and then fixed supine with a clamping device, which was mounted on a stage allowing for translational displacements in all spatial directions plus one rotational degree of freedom. A thin brass plate, fixed on the ventral side of the prosoma, restrained the spider and prevented liberation in a ventral direction. The spider's second leg was immobilized in the range of the proximal tibia. A small steel hook was connected near the distal end of the metatarsus and connected free of play to a muscle lever system (Aurora Scientific Inc., 300B-LR; lever arm length: 30 mm; r_{hook} : distance between the hook and the tibia–metatarsus joint). The lever enabled control of either force F_{Lev} or excursion L_L during tibia–metatarsus joint flexion (sample rate: 1000 Hz).

Efferent nerves innervate the tibia–metatarsus joint flexors originating from the main leg nerve bundle distally of the patella (Ruhland and Rathmayer 1978; Seyfarth et al. 1985). The ventral patella, where the nerve is located directly beneath the cuticula, was punctured distally and proximally with two needle electrodes. Haemolymph coagulation sealed the penetration sites within seconds.

The flexor muscles were stimulated supramaximally by 1 mA current pulses with 100 μ s duration. To minimize fatigue, the frequency was adjusted such that fused tetanic contractions occurred (fusion frequency 120–140 Hz). Burst duration was 300 ms during isometric experiments and 500 ms during isotonic experiments. Rest between contractions was 120 s, which was sufficient to avoid fatigue.

After the fixation phase, the spiders recovered from the anesthesia but were not anaesthetized during the experiments. Subsequent to experiments, the released spiders' leg function seemed to be unimpaired.

Estimation of tibia–metatarsus joint angle and moment

Preceding each experiment, the spider was arranged such that the hook was perpendicular to the metatarsus ($\beta = 90^\circ$) and to the motor lever arm ($\gamma = 90^\circ$, Fig. 1a). The length of the motor lever arm was assumed to be constant during its rotation ($\Delta\gamma \pm 9^\circ$), thereby introducing a small error in F_{Lev} (max $\pm 1.2\%$). However, r_{hook} was much smaller than both the motor lever arm (threefold r_{hook}) and the hook length (fourfold r_{hook}). Thus, the perpendicular distance between the line of action of F_{Lev} and the tibia–metatarsus joint, $r_{hook\perp}$, shortened considerably during lever arm rotation and could be approximated with:

$$r_{hook\perp} = \sqrt{r_{hook}^2 - L_L^2} \tag{1}$$

The tibia–metatarsus joint moment equaled

$$M = F_{Lev} \cdot r_{hook\perp}, \tag{2}$$

and the joint angle α was approximated as

$$\alpha = \alpha_0 - \text{asin}(L_L/r_{hook}), \tag{3}$$

where α_0 is the joint angle at the initial position. For every experiment with spiders S1–S5, initial L_{met} , r_{hook} and α_0 were measured from a photograph perpendicular to the joint movement plane.

Geometric functions

In spiders S7–S9 of a rather similar size ($L_{met7-9} = 11.2 \pm 0.3$ mm), the dependence of the muscle lever $r_{m\perp}$ and the muscle length change ΔL_m on the joint angle α (Fig. 1b) was measured with a microscope (20 \times , Zeiss

Stemi 2000, equipped with a micrometer eyepiece) in roughly 20° steps from 85° to 205°. Assuming geometric similarity for the legs of *Cupiennius salei* (Prange 1977), the $r_{m\perp}$ and ΔL_m of the spiders S1–S5 were calculated by scaling with respect to individual L_{met} .

The muscle is assumed to insert via an articulate joint membrane (m_1) on the ventral corner of the proximal metatarsus border (m_2) pulling in parallel to the longitudinal axis of the tibia (Fig. 1b). Then, $r_{m\perp}$ is the perpendicular distance between the muscle force vector and the joint axis (Fig. 1b). m_1 and m_2 are observable markers during joint flexion from 210° to $\approx 100^\circ$. Further flexion to 80° leads to covering of m_1 by the distal tibia border and the muscle force vector was approximated to end in m_2 . The $r_{m\perp}$ –angle [°] relations of the three spiders were fitted with a single parabolic function (Fig. 2a):

$$r_{m_fit\perp}(\alpha) = 0.9425 \times 10^{-4} \cdot \alpha^2 + 0.0281 \cdot \alpha - 1.1575 \tag{4}$$

The $r_{m\perp}$ of the spiders S1–S5 was estimated using their individual L_{met} and L_{met7-9} :

$$r_{m\perp} = r_{m_fit\perp} \cdot \frac{L_{met}}{L_{met7-9}}. \tag{5}$$

The muscle length change ΔL_m was measured as the distance in tibia direction between muscle insertion (m_1) and the ventral corner of the distal tibia border (Fig. 1b, m_3). Joint flexion larger than 100° led to covering of m_1 . In these situations, ΔL_m was approximated as the distance in tibia direction between m_2 and m_3 , and which was offset by the length of the joint membrane (Fig. 1b). The resulting ΔL_m – joint angle [°] relations were fitted with a linear function (Fig. 2b):

$$\Delta L_{m_fit}(\alpha) = 0.0155 \cdot \alpha - 1.5866 \tag{6}$$

Individual ΔL_m of spiders (S1–S5) were estimated as

$$\Delta L_m = \Delta L_{m_fit} \cdot \frac{L_{met}}{L_{met7-9}}. \tag{7}$$

Fig. 1 a Schematic of the experimental setup. The motor lever arm is approximately $3 \times r_{hook}$. **b** Geometry model of the tibia–metatarsus joint. White circles show articulated structures. For details see text

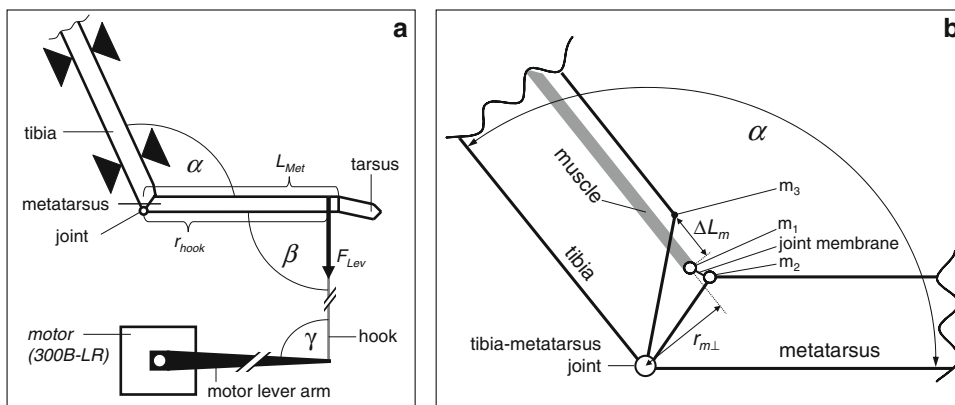
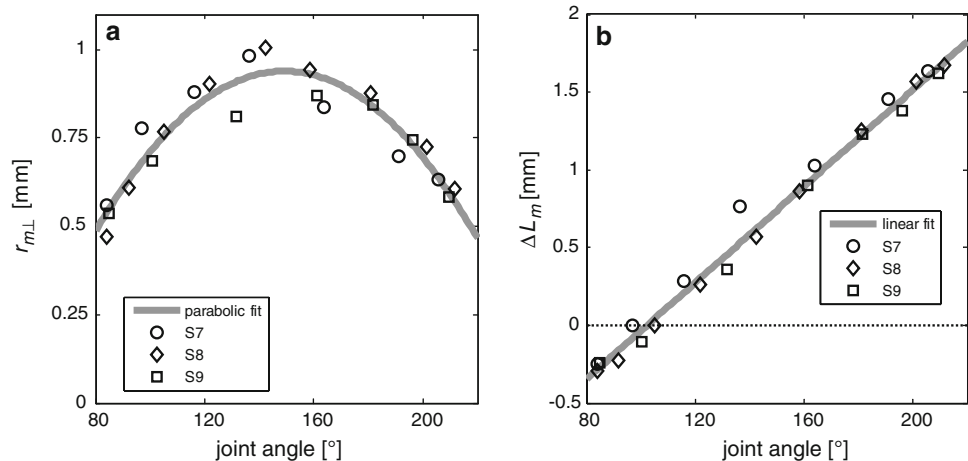


Fig. 2 Dependency of: **a** The muscle lever $r_{m\perp}$ and the joint angle α ; **b** the muscle length change ΔL_m and the joint angle α . The coefficients of determination R^2 between measured (symbols) and fitted (gray lines) data were 0.88 for (a) and 0.99 for (b). The parabolic function decreases $r_{m,fit\perp}$ by less than 5% for joint angles from 126 to 174°



Calculation of muscle force and muscle length

Muscle force is given by

$$F_m = \frac{M}{r_{m\perp}}. \quad (8)$$

To approximate muscle length, we determined a mean value of previously published relative (to metatarsus length) muscle fascicle lengths at a 90° joint angle (0.39 ± 0.2 ; Blickhan and Barth 1985, adapted from Fig. 11a). Muscle length was calculated as the sum of the muscle fiber length at 90° and muscle length change due to joint angle change:

$$L_m = 0.39 \cdot L_{met} + \Delta L_m(\alpha) - \Delta L_m(90^\circ). \quad (9)$$

Experiments

The passive and the total (during activation) moment–angle relation was determined by a set of isometric contractions at joint angles ranging from 85° to 200° in steps of about 20°. Since the passive moment resulted from the ventral hinge stop and the dorsal limit, but not from the muscle (checked on isolated muscle), passive moment (measured before stimulation) could simply be subtracted from the total moment (corresponding to the maximum force during stimulation) to obtain the active moment.

The force–velocity relationship was determined by a combination of isotonic experiments (Fenn and Marsh 1935; Till et al. 2008) and step-and-ramp shortening experiments (Curtin et al. 1998; Siebert et al. 2008). While the first method yields one force–velocity data point per trial, the latter ensures measurement at high shortening velocities with a fully activated muscle. However, with one disadvantage: the experiment must be conducted an average of two or three times before one data point can be obtained (Curtin et al. 1998). The combination of the two methods minimizes the number of experiments required to obtain a complete force–velocity relationship, thereby avoiding fatigue.

Isotonic experiments were started at about 170° joint angle, an angle sufficient to yield maximal velocities during shortening at about the optimal muscle length. The contractions were performed at tensions of approximately 0.15 maximum isometric force (F_{im}) in steps of 0.15 F_{im} up to a tension with no concentric movement. The isotonic force of each experiment was normalized to the force of the preceding isometric reference-contraction to yield the normalized force–velocity value.

Step-and-ramp shortening experiments (Fig. 3a: given angle–time traces, Fig. 3b: resulting force–time traces) started with a 300 ms isometric pre-stimulation sufficient to reach an isometric force plateau (Fig. 3b) and hence full activation during the subsequent shortening phase. In six to eight experiments with velocities ranging from $0 < v < v_{max}$, the step distance was adjusted such that force transients in the isokinetic ramp part were minimized. Starting from about 170° tibia–metatarsus joint angle (Fig. 3), constant force was reached at optimum muscle length. This force was normalized to the isometric force preceding shortening to yield the normalized force–velocity value.

Isometric reference contractions at optimum muscle length were performed throughout the experiments. Force loss due to fatigue was less than 5% during the isometric experiments and less than 10% during the determination of the force–velocity relationship.

Muscle model

The determined force–velocity values were approximated with the Hill hyperbola (Hill 1938) for concentric contractions

$$f_v(v) = \frac{v_{max} - v}{v_{max} + v/curv}, \quad (10)$$

where f_v is a percentage of the maximum isometric force F_{im} , v_{max} is the maximal shortening velocity and $curv$ (in

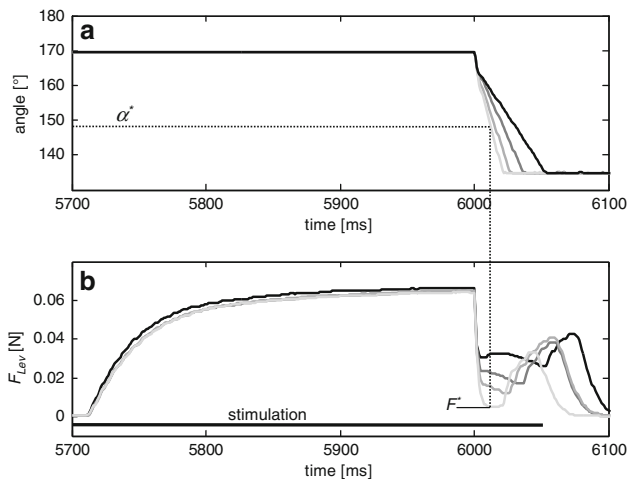


Fig. 3 Four examples of S5 step-and-ramp shortening experiments with different step distances and shortening velocities (*lines with different gray scales*). **a** angle-time traces and **b** resulting lever force-time traces. A constant force phase occurred within the plateau range of the muscle force-length relation ($145^\circ < \alpha^* < 190^\circ$). F^* is the corresponding force yielding the f_v value when normalized to F_{im} and is shown exemplarily for the ramp with the highest shortening velocity

the literature also denoted as a/F_{im} , where a is a typical Hill-parameter) defines the curvature of the relationship.

The determined isometric force-length values were approximated with a parabola (Woittiez et al. 1984)

$$F_1(L_m) = F_{im} \cdot \left(1 - \left(\frac{L_m - L_{mopt}}{w} \right)^2 \right), \quad (11)$$

where L_{mopt} is the optimum muscle length, w is the depth of the parabola, and L_m is the muscle length. The plateau of the parabola was defined as the length range where $F_1 \geq 0.95F_{im}$. Moment-angle parameters were determined with Eq. (11) substituting F_{im} with maximum isometric moment M_{im} , L_m with α , L_{mopt} with optimum angle α_{opt} , and w with depth of the parabola in degree w_{deg} .

Results

In the 90° – 195° joint angle range, passive, quasi-static joint moments were negligible ($< 2\%$ maximum active moment). The ventral hinge stop at about 85° and the dorsal limit at about 200° restrict the anatomical joint range. Flexion from 90° increases passive negative moment, and extension from 195° increases passive positive joint moment.

The homogeneous active moment-angle relations of the S1–S5 tibia-metatarsus joints (Fig. 4) are approximately parabolic. Maximum active isometric moments occur at the optimum joint angle $159.3 \pm 6.9^\circ$ (Table 1). Further extension decreases the isometric moment. However, when

extrapolated from the parabolic fits at the overextended 200° angle, the moment is still $71.5 \pm 13.0\%$ of the maximum isometric moment. In contrast, isometric moments are low ($11.0 \pm 11.0\%$) close to the hinge stop at 85° .

Applying the geometry function (Eq. 4), approximate parabolic force-length relationships (Fig. 5) are derived from the moment-angle relations (Fig. 4). Muscle lengths (Fig. 5, dotted vertical lines) related to optimal joint angles are near the optimal muscle length. Muscles reach their optimal length at 6.5 ± 0.6 mm and produce a maximum isometric force of 0.61 ± 0.05 N (Table 1).

The force-velocity relationships exhibit the typical hyperbolic shape (Fig. 6). The maximum shortening velocity is 36.7 ± 6.8 mm/s corresponding to 5.7 ± 1.3 [muscle length/s], and the curvature of the Hill-function is 0.34 ± 0.07 (Table 1). The joint angle and the muscle's length change are linearly related (Fig. 2b) and $r_{m\perp}$ remains rather constant during the force-velocity experiments. Hence, the moment-angular velocity relation and the force-velocity relationship have identical curv values, and the angular velocity is $\omega = kv$, where $k = \omega_{max}/v_{max} = 52.3 \pm 3.6^\circ/\text{mm}$.

Discussion

Geometric model

In contrast to the slightly nonlinear dependency between extensor tibiae muscle length and joint angle of stick insects (Guschlbauer et al. 2007), the spider muscle length depends linearly on the joint angle in the range of motion. Additionally, in the range of 126° – 174° , the change in muscle lever length is negligible (Fig. 2). As a result, the muscle has nearly optimal length at the optimal joint angle (Fig. 5).

Impact on locomotion

Kinematic analysis of running *Cupiennius salei* has shown that the tibia-metatarsus joint angle is about 90° during the last fourth of the stance phase (Reinhardt 2006). Moreover, the ground reaction forces create low flexing moments in this phase (Weihmann and Blickhan 2006). The results of our study suggest that these low moments may be compensated by passive joint moments resulting from the ventral hinge stop.

In contrast to skeletal muscles with high passive forces within the anatomical range (e.g., $0.2 F_{im}$ in cat *M. soleus*, Rode et al. 2009), the spider muscle has negligible passive muscle force enabling facile hydraulic joint extension up to the dorsal limit.

Fig. 4 Measured (black dots) moment–angle values and fitted (gray line) moment–angle relations of spiders S1–S5. An exemplary passive moment–angle relationship (crosses) is shown for S1

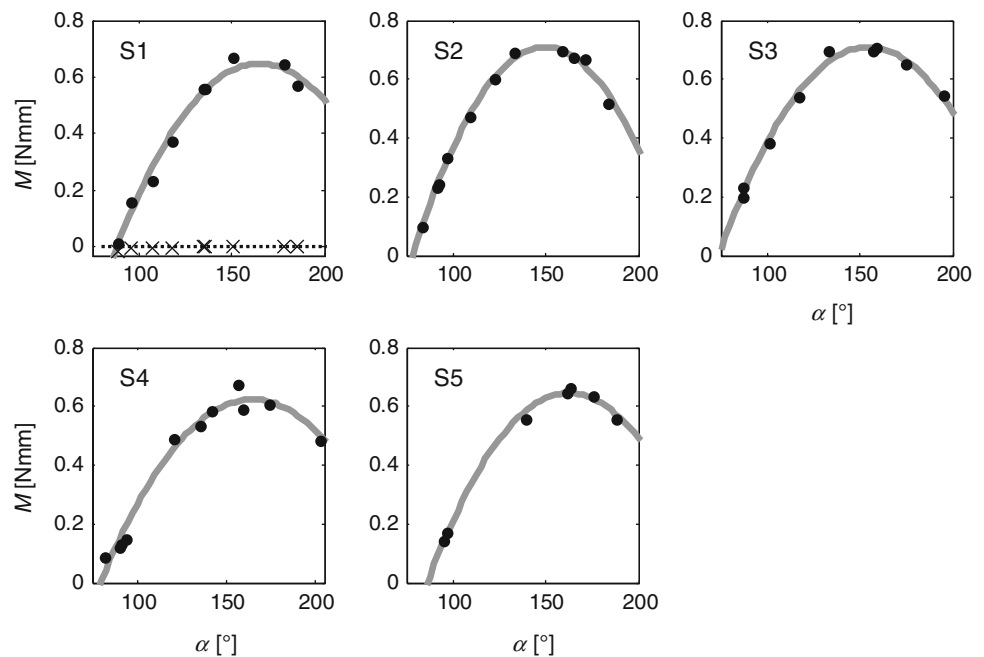


Table 1 Tibia–metatarsus joint parameters and muscle properties of the spiders S1–S5

Relation	Variable	S1	S2	S3	S4	S5	MW	STD
Moment–angle	L_{met} (mm)	12.8	12.8	13.4	14.5	11.8	13.1	1.0
	M_{im} (Nmm)	0.64	0.71	0.71	0.63	0.64	0.67	0.04
	α_{opt} (°)	165.1	149.6	154.6	164.9	162.6	159.3	6.9
	w_{deg} (°)	77.0	71.5	80.8	85.5	76.4	78.2	5.2
Force–length	F_{im} (N)	0.60	0.66	0.61	0.53	0.65	0.61	0.05
	L_{mopt} (mm)	6.4	6.0	6.5	7.5	5.9	6.5	0.6
	w (mm)	1.5	1.4	2.0	2.3	1.6	1.7	0.4
Force–velocity	v_{max} (mm/s)	29.5	47.7	37.4	36.0	33.0	36.7	6.8
	$v_{\text{max}} (L_{\text{mopt}}/s)$	4.6	7.9	5.8	4.8	5.6	5.7	1.3
	ω_{max} (°/s)	1,588	2,476	1,931	1,703	1,885	1,917	342
	$curv$	0.32	0.24	0.38	0.35	0.43	0.34	0.07
	p_{max} (mW)	1.95	2.91	2.74	2.16	2.67	2.48	0.41

Additionally, metatarsus lengths are given for all spiders

Many vertebrate muscles which are relevant for propulsion shorten at about one-third v_{max} to produce peak power at the preferred speeds of the animal (Rome et al. 1988; Lutz and Rome 1996; Biewener 1998). Similar results were found for the cockroach muscle 177c, which shortens with $0.33 v_{\text{max}}$ at 0.25 m/s running (Ahn and Full 2002). The contractile speed for maximum efficiency is slightly below that for maximum power (e.g., Woledge 1998). During running at 0.3 m/s, in *Cupennius salei*, the maximal angle velocity of the tibia–metatarsus joint is about 750°/s (Reinhardt 2006). This corresponds to a $0.25 v_{\text{max}}$ muscle shortening velocity. Hence, like the cockroach muscle 177c, the flexor muscle could act as an efficient motor during the stance phase of locomotion. Seemingly, at

preferred locomotion speed, arthropod muscles, as well as vertebrate muscles shorten at one-third v_{max} .

Ahn and Full (2002) could demonstrate, that, during cockroach running, muscles within a muscle group may differ in that they absorb or deliver energy during locomotion. Detailed recordings of muscle activity of the separate spider muscles (FML, FMA, FMB) during locomotion are not available. In addition, rigorous assessment of the in vivo function of the separate muscles during locomotion would require direct determination of isolated muscle forces under in vivo stimulation and strain conditions. The classification of the spider musculature examined as a motor is based on the observed flexion of the tibia–metatarsus joint during the stance phase (Reinhardt

Fig. 5 Muscle force–length values (black points) derived from the measured moment–angle values and the fitted force–length relationships (gray line) of spider’s (S1–S5) second leg pair. Dotted lines indicate muscle lengths corresponding to optimal joint angles. The length-axis range of the figures corresponds to the Fig. 4 joint angle range

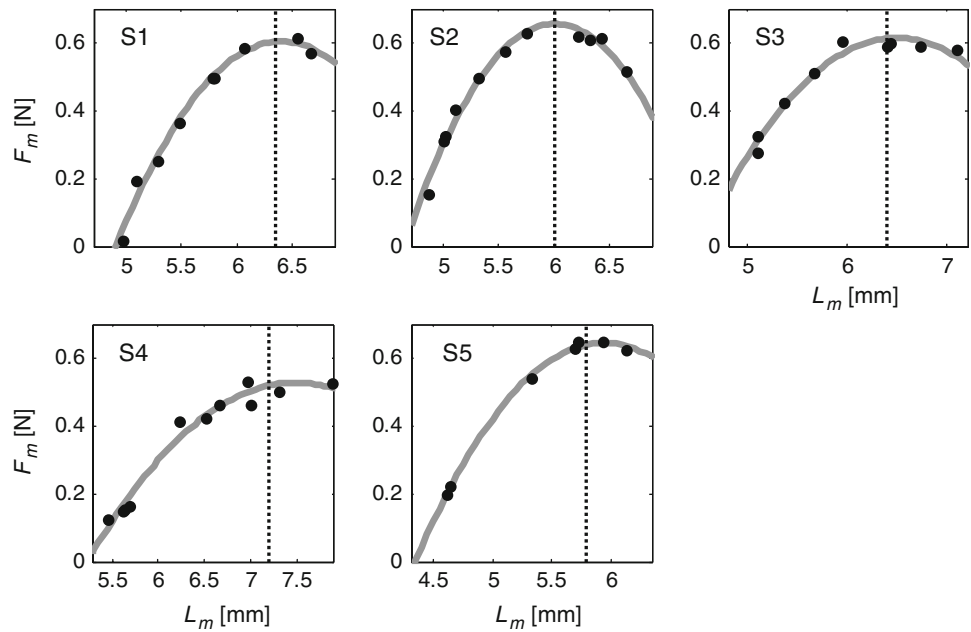
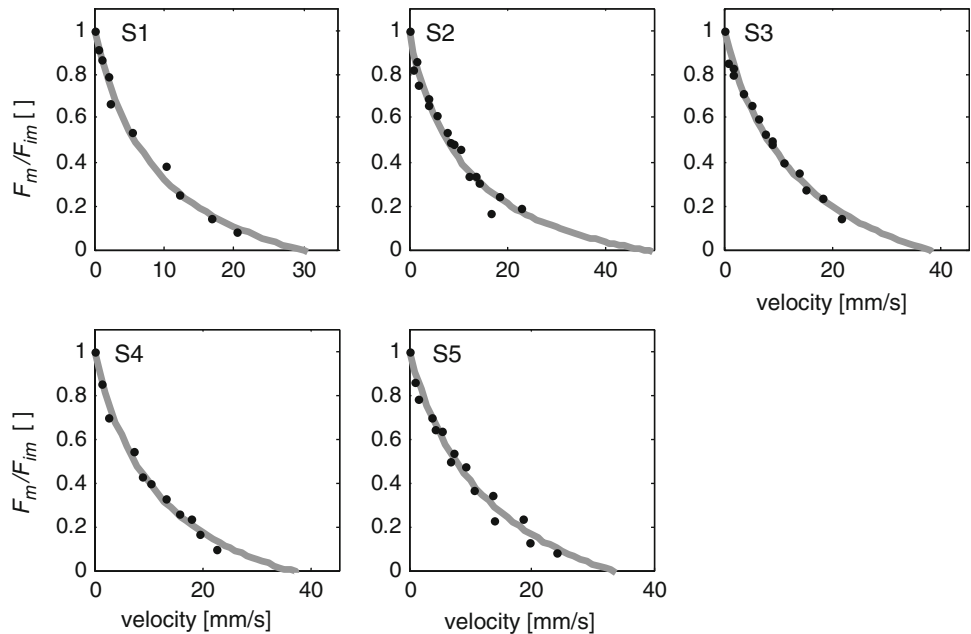


Fig. 6 Force–velocity relationships of the specimens S1–S5. The fitted hyperbolic force–velocity relationship (gray line) approximates the force–velocity values (black points) determined from measured moment–angle velocity values



2006), and on the assumption that the three flexor muscles (FML, FMA, FMB) contribute as synergists to this joint flexion.

Due to their intrinsic mechanical properties, muscles may help stabilize the muscle–skeletal system (Brown and Loeb 2000). Brown and Loeb (2000) termed the muscle’s zero-delay response to a perturbation “preflex”. Kinematic analyses of running *Cupiennius salei* have shown that the tibia–metatarsus joint of the second leg flexes from 131° to 90° during the stance phase (Reinhardt 2006). Thus, during running, the muscle works on the ascending limb of the moment–angle relation (Fig. 4) and the force–length

relation (Fig. 5). The same was reported for e.g., stick insect extensor tibiae (Guschlbauer et al. 2007), for cat *M. soleus* (Herzog et al. 1992), for human *M. tibialis anterior*, *M. soleus* (Maganaris 2001), *M. gastrocnemius medialis* (Maganaris 2003) and for human *M. biceps brachii* (Leedham and Dowling 1995) all of which when put under static conditions result in a self-stabilizing effect of the muscle properties (Wagner and Blickhan 1999). This effect may allow a static spider standing on a leaf to come back to its initial position after it has been blown by the wind or after the leaf has moved without exercising neural control. Furthermore, there are hints that the ascending

limb of the force–length relations contributes to the self-stabilization of the system under dynamic conditions (Wagner and Blickhan 1999, 2003). Accordingly, this may reduce neural control during spider locomotion on bumpy ground and unstable substrate.

Comparison of muscle properties

Only a few invertebrate studies have been published and, to our knowledge, no dynamic spider muscle properties have been investigated. For this reason, we searched the literature for arthropod leg muscles which also contribute to terrestrial locomotion, and whose properties were determined in similar experiments *in situ* [fused tetanic contractions, similar temperature, complete set of Hill-parameters: cockroach (Ahn and Full 2002); stick insect (Guschlbauer et al. 2007)]. As an additional example, we selected a katydid wing muscle (Josephson 1984, 1993) operating at a stroke frequency of 20 Hz, which is slightly above the maximal spider step frequency (~ 10 Hz, Blickhan et al. 2005).

The cockroach muscles 179 and 177c extend the coxa–femur joint. Muscle 177c operates like a motor, producing mechanical energy to extend the hind limb, while muscle 179 acts as a brake, actively absorbing mechanical energy to slow down flexion. In the walking stick insect, the *M. extensor tibialis* extends the femur–tibia joint during leg swing. The katydid wing muscle runs from the tergum to the anterior coxa and is used as a flight muscle. All spider muscle properties examined are very similar to muscle 177c properties (Table 2). Their maximum stress is in the

range of the average 30 N/cm^2 maximum stress produced by mammalian muscles (Alexander 1985). In comparison to the spider muscle, the cockroach muscle 179 is stronger, whereas the stick insect muscles and the katydid muscles are much weaker. *Curv* and normalized v_{max} are similar for both the cockroach and spider muscles. However, whereas the stick insect muscle's *curv* value is in the same range as the spider's value, its v_{max} is only half the spider's value.

Mammalian muscle's force–velocity parameters are related to their fiber type. To date, no histochemical study regarding the fiber type distribution of *Cupiennius salei* tibia–metatarsus flexors is available. The comparison of its force–velocity parameters with parameters from the literature might allow the prediction of the predominant fiber type. In mammals, v_{max} ranges from $20 L_{\text{mopt}}/\text{s}$ for the fast twitch fibered rat *M. extensor digitorum longus* (Ranatunga and Thomas 1990), to $3 L_{\text{mopt}}/\text{s}$ for the slow twitch fibered cat *M. soleus* (Scott et al. 1996; Siebert et al. 2008). Moreover, *curv* is higher for fast muscles than for slow ones (Close 1972; Josephson 1984). Fast insect muscles achieve similar v_{max} to mammalian muscles (Josephson 1984, Table 2), whereas the spider muscle's v_{max} is rather similar to mammalian slow twitch muscles. The *curv* value, however, is similar to fast twitch mammalian muscles (e.g., rat *M. extensor digitorum longus*, *curv* = 0.31, Ranatunga and Thomas 1990). Thus, the results of this study do not allow a clear prediction of the fiber type of the spider muscle examined.

For general comparison of muscle properties (particularly maximum muscle stress) among different species or muscles, usage of fused tetanic contractions is widespread (e.g.,

Table 2 Characteristic arthropod muscle properties: cockroach (Ahn and Full 2002), stick insect (Guschlbauer et al. 2007), cone-headed katydid (Josephson 1984, 1993) and spider muscle properties that were determined

	Cockroach <i>Blaberus discoidalis</i>		Stick insect <i>Carausius morosus</i> Extensor tibialis	Cone-headed katydid <i>Neoconocephalus triops</i> Metathoracic tergo-coxal wing muscle		Spider <i>Cupiennius salei</i> Flexor muscle
	Muscle 179	Muscle 177c				
Max. stress (N/cm^2)	47	26	7.9	12.2	11.8	25.3*
F_{im} (N)	0.4*	0.6*	0.15	0.12*	0.12*	0.61
v_{max} (mm/s)	20.6	49.2	4.4	100*	67.9*	36.7
v_{max} (L_{mopt}/s)	4.9	5.7	3.1	17.0	11.6	5.7
L_{mopt} (mm)	4.1	9	1.4*	5.9	5.9	6.5
<i>curv</i>	0.6	0.5	0.39	0.9	–	0.34
temperature ($^{\circ}\text{C}$)	25	25	20–22	35	25	20–22
Stimulation frequency (Hz)	200	200	200	400	400	120–140

In addition, temperature during experiments and stimulation frequency resulting in fused tetanic contractions are given. For the katydid muscle, the left and right columns correspond to 35 and 25°C , respectively

* Calculated values. Underlying assumptions: muscle volume = $l_{\text{mopt}} \times \text{cross sectional area (CSA)}$ = muscle mass / muscle density (muscle density = 1.056 g/cm^3 , Mendez and Keys 1960). Muscle mass was given in the cited literature. For the spider, muscle volume was assumed to be concordant with tibia volume (Blickhan and Barth 1985). Maximum stress is F_{im}/CSA

Wells 1965; Herzog et al. 1992; Baratta et al. 1995; Edman 2005; Wagner et al. 2005). However, stimulation frequency (Joyce et al. 1969; Brown et al. 1999; Guschlbauer et al. 2007) and temperature (Bennett 1985) influence the muscle properties. In contrast to the spider data which was determined at fusion frequency, cockroach and stick insect data were collected from stimulation frequencies exceeding the fusion frequency (Ahn and Full 2002; Guschlbauer et al. 2007; Josephson 1984). Whereas, maximum isometric force increased only marginally at higher stimulation frequencies, stimulation frequencies exceeding fusion frequency clearly increased forces at high shortening velocities in rats *M. gastrocnemius medialis* (de Haan 1998). For the stick insect muscle, high stimulation frequencies ($2.5\times$ fusion frequency) lead to an increase of about 15% in maximum shortening velocity (Guschlbauer et al. 2007). The curvature of the force–velocity relations seems to be independent of stimulation frequency (Guschlbauer et al. 2007). Therefore, while other Hill-parameters might be unaffected by stimulation frequencies exceeding fusion frequency, the maximum shortening velocities of the spider muscles may be underestimated in comparison with those of other arthropod muscles (Table 2).

In arthropods, peripheral inhibition is generally reported for slow fibers (Rathmayer 1990, 1996) and was demonstrated in several leg muscles (e.g., claw muscles in *Cupiennius salei*, Maier et al. 1987; flexor muscles in the stick insect, Guschlbauer et al. 2007). Coactivation of fast and slow muscle fibers decreases force development and increases muscle relaxation time (Rathmayer 1990, 1996). Therefore, peripheral inhibition of the slow fibers enables faster contraction and relaxation of the whole muscle (Rathmayer 1990, 1996).

In tarantulas, the tibia–metatarsus joint flexors are not innervated by such inhibitory axons (Rathmayer 1965; Zebe and Rathmayer 1968; Sherman 1985). For *Cupiennius salei*, no examination of inhibitory axons exists. However, due to the small contribution of inhibited slow fibers to muscle cross sectional area, the influence on the contraction dynamics of the almost fully stimulated arthropod muscle should be negligible (Maier et al. 1987; Rathmayer 1990, 1996).

Fast running with relatively slow contracting muscles?

Adult female *Cupiennius salei* reach a maximum sprint velocity of 0.7 m/s (Blickhan et al. 2005) corresponding to about 20 [body length/s]. Therefore, with a velocity ratio of 4.7 (maximum velocity/mass^{0.33}, Full and Ahn 1995), they can be characterized as fast runners. In contrast, we found relatively slow ($v_{\max} = 5.7 L_{\text{mopt}}/s$) contracting muscles flexing the tibia–metatarsus joint. How can this be reconciled with fast running spiders?

Spiders have long legs in comparison to prey of a similar size (similar body mass). In addition, the mechanical advantage (Biewener 1989; Full and Ahn 1995) in the examined joint (muscle lever/metatarsus length = 1/13) is relatively low. Thus, even a slow, but sufficiently strong muscle can invoke high velocities at the distal tip of the leg segment. Unlike all other arthropods, in spiders almost the entire tibia is filled with flexor muscles (Blickhan and Barth 1985) thereby maximizing the flexing force within rather slender legs.

Moreover, in the leg examined, the speed at the leg's tip is generated by the superposition of segment velocities created by several joints turning in the same direction. The more joints are arranged in series, the slower the individual joint's rotational velocities may be when creating a desired leg-tip velocity. Indeed, the spider leg is constructed such that there are three actuated joints in series, which decreases the necessary contractile speed of the muscles.

Acknowledgments We thank the German Science Foundation (DFG) for support of work (Bl 236/14-2).

References

- Ahn AN, Full RJ (2002) A motor and a brake: two leg extensor muscles acting at the same joint manage energy differently in a running insect. *J Exp Biol* 205:379–389
- Ahn AN, Meijer K, Full RJ (2006) In situ muscle power differs without varying in vitro mechanical properties in two insect leg muscles innervated by the same motor neuron. *J Exp Biol* 209:3370–3382
- Alexander RM (1985) The maximum forces exerted by animals. *J Exp Biol* 115:231–238
- Anderson JF, Prestwich KN (1975) The fluid pressure pumps of spiders (Chelicerata, Araneae). *Z Morph Tiere* 81:257–277
- Baratta RV, Solomonow M, Best R, Zembo M, D'Ambrosia R (1995) Force–velocity relations of nine load-moving skeletal muscles. *Med Biol Eng Comput* 33:537–544
- Bennett AF (1985) Temperature and muscle. *J Exp Biol* 115:333–344
- Biewener AA (1989) Scaling body support in mammals: limb posture and muscle mechanics. *Science* 245:45–48
- Biewener AA (1998) Muscle function in vivo: a comparison of muscles used for elastic energy storage savings versus muscles used to generate power. *Am Zool* 38:703–717
- Blickhan R, Barth FG (1985) Strains in the exoskeleton of spiders. *J Comp Physiol A* 157:115–147
- Blickhan R, Wagner H, Seyfahrt A (2003) Brain or muscles? *Recent Res Devel Biomech* 1:215–245
- Blickhan R, Petkun S, Weihmann T, Karner M (2005) Schnelle Bewegungen bei Arthropoden: Strategien und Mechanismen. In: Pfeiffer F, Cruse H (eds) *Autonomes Laufen*. Springer, Berlin, pp 19–45
- Blickhan R, Seyfahrt A, Geyer H, Grimmer S, Wagner H, Gunther M (2007) Intelligence by mechanics. *Philos Transact A Math Phys Eng Sci* 365:199–220
- Brown IE, Loeb GE (2000) A reductionistic approach to creating and using neuro-musculoskeletal models. In: Winters JM, Crago PE (eds) *Biomechanics and neural control of posture and movement*. Springer, New York

- Brown IE, Cheng EJ, Loeb GE (1999) Measured and modeled properties of mammalian skeletal muscle. II. The effects of stimulus frequency on force–length and force–velocity relationships. *J Muscle Res Cell Motil* 20:627–643
- Clarke J (1986) The comparative functional morphology of the leg joints and muscles of five spiders. *Bull Brachnol Soc* 7:37–47
- Close RI (1972) Dynamic properties of mammalian skeletal muscles. *Physiol Rev* 52:129–197
- Curtin NA, Gardner-Medwin AR, Woledge RC (1998) Predictions of the time course of force and power output by dogfish white muscle fibres during brief tetani. *J Exp Biol* 201:103–114
- de Haan A (1998) The influence of stimulation frequency on force–velocity characteristics of in situ rat medial gastrocnemius muscle. *Exp Physiol* 83:77–84
- Dillon LS (1952) The myology of the araneid leg. *J Morphol* 90:467–480
- Edman KA (2005) Contractile properties of mouse single muscle fibers, a comparison with amphibian muscle fibers. *J Exp Biol* 208:1905–1913
- Ehlers M (1939) Untersuchungen über Formen aktiver Lokomotion bei Spinnen. *Zool Jb Syst* 72:373 ff
- Ellis CH (1944) The mechanism of extension in the legs of spiders. *Biol Bull* 86:41–50
- Fenn WO, Marsh BS (1935) Muscular force at different speeds of shortening. *J Physiol* 85:277–297
- Full R, Ahn A (1995) Static forces and moments generated in the insect leg: comparison of a three-dimensional musculo-skeletal computer model with experimental measurements. *J Exp Biol* 198:1285–1298
- Gordon AM, Huxley AF, Julian FJ (1966) The variation in isometric tension with sarcomere length in vertebrate muscle fibres. *J Physiol* 184:170–192
- Guschlbauer C, Scharstein H, Buschges A (2007) The extensor tibiae muscle of the stick insect: biomechanical properties of an insect walking leg muscle. *J Exp Biol* 210:1092–1108
- Herzog W, Leonard TR, Renaud JM, Wallace J, Chaki G, Bornemisza S (1992) Force–length properties and functional demands of cat gastrocnemius, soleus and plantaris muscles. *J Biomech* 25:1329–1335
- Hill AV (1938) The heat of shortening and the dynamic constants of muscle. *Proc R Soc London Ser B, Biol Sci* 126:136–195
- Josephson RK (1984) Contraction dynamics of flight and stridulatory muscles of tettigoniid insects. *J Exp Biol* 108:77–96
- Josephson RK (1993) Contraction dynamics and power output of skeletal muscle. *Annu Rev Physiol* 55:527–546
- Joyce GC, Rack PM, Westbury DR (1969) The mechanical properties of cat soleus muscle during controlled lengthening and shortening movements. *J Physiol* 204:461–474
- Leedham JS, Dowling JJ (1995) Force–length, torque–angle and EMG–joint angle relationships of the human in vivo biceps brachii. *Eur J Appl Physiol Occup Physiol* 70:421–426
- Lutz GJ, Rome LC (1996) Muscle function during jumping in frogs. II. Mechanical properties of muscle: implications for system design. *Am J Physiol* 271:C571–578
- Maganaris CN (2001) Force–length characteristics of in vivo human skeletal muscle. *Acta Physiol Scand* 172:279–285
- Maganaris CN (2003) Force–length characteristics of the in vivo human gastrocnemius muscle. *Clin Anat* 16:215–223
- Maier L, Root TM, Seyfarth EA (1987) Heterogeneity of spider leg muscle: histochemistry and electrophysiology of identified fibers in the claw levator. *J Comp Physiol B, Biochem Syst Environ Physiol* 157:285–294
- Melchers M (1967) Der Beutefang von *Cupiennius salei* Keyserling (Ctenidae). *Z Morph Ökol Tiere* 58:321–346
- Mendez J, Keys A (1960) Density and composition of mammalian muscle. *Metabolism* 9:184–188
- Moya-Larano J, Vinkovic D, De Mas E, Corcobado G, Moreno E (2008) Morphological evolution of spiders predicted by pendulum mechanics. *PLoS ONE* 3:e1841
- Parry DA, Brown RHJ (1959) The hydraulic mechanism of the spider leg. *J Exp Biol* 36:423–433
- Prange HD (1977) The scaling and mechanics of arthropod exoskeletons. In: Pedley TJ (ed) *Scale effects in animal locomotion*. Academic Press, London, pp 169–181
- Ranatunga KW, Thomas PE (1990) Correlation between shortening velocity, force–velocity relation and histochemical fibre-type composition in rat muscles. *J Muscle Res Cell Motil* 11:240–250
- Rathmayer W (1965) Neuromuscular transmission in a spider and the effect of calcium. *Comp Biochem Physiol* 14:673
- Rathmayer W (1990) Inhibition through neurons of the common inhibitory type (CI-neurons) in crab muscle. In: Krentz WD, Tautz J, Reichert H, Mulloney B, Wiese K (eds) *Frontiers in crustacean neurobiology*. Birkhäuser, Basel, pp 271–278
- Rathmayer W (1996) Motorische Steuerung bei Invertebraten. In: Dudel J, Menzel R, Schmidt RF (eds) *Neurowissenschaft*. Springer, Berlin, pp 167–190
- Reinhardt L (2006) Gleichförmige Lokomotion der Jagdspinne *Cupiennius salei* (KEYSERLING 1877): 3D-Beinsegmentkinematik. Thesis, Friedrich-Schiller-University, Jena
- Rode C, Siebert T, Herzog W, Blickhan R (2009) The effects of parallel and series elastic components on the active cat soleus force–length relationship. *J Mech Med Biol* 9:105–122
- Rome LC, Funke RP, Alexander RM, Lutz G, Aldridge H, Scott F, Freadman M (1988) Why animals have different muscle fibre types. *Nature* 335:824–827
- Ruhland M, Rathmayer W (1978) Die Beinmuskulatur und ihre Innervation bei der Vogelspinne *Dugesiella hentzi* (Ch.) (Araneae, Aviculariidae). *Zoomorphology* 89:33–46
- Scott SH, Brown IE, Loeb GE (1996) Mechanics of feline soleus: I. Effect of fascicle length and velocity on force output. *J Muscle Res Cell Motil* 17:207–219
- Seyfarth EA, Eckweiler W, Hammer K (1985) Proprioceptors and sensory nerves in the legs of a spider, *Cupiennius salei* (Arachnida, Araneida). *Zoomorphology* 105:190–196
- Sherman RG (1985) Neural control of the heartbeat and skeletal muscle in spiders and scorpions. In: Barth FG (ed) *Neurobiology of arachnids*. Springer, Berlin, pp 319–336
- Siebert T, Sust M, Thaller S, Tilp M, Wagner H (2007) An improved method to determine neuromuscular properties using force laws—from single muscle to applications in human movements. *Hum Mov Sci* 26:320–341
- Siebert T, Rode C, Herzog W, Till O, Blickhan R (2008) Nonlinearities make a difference: comparison of two common Hill-type models with real muscle. *Biol Cybern* 98:133–143
- Stewart DM, Martin AW (1974) Blood pressure in the tarantula *Dugesiella hentzi*. *J Comp Physiol* 88:141–172
- Till O, Siebert T, Rode C, Blickhan R (2008) Characterization of isovelocity extension of activated muscle: a Hill-type model for eccentric contractions and a method for parameter determination. *J Theor Biol* 255:176–187
- Wagner H, Blickhan R (1999) Stabilizing function of skeletal muscles: an analytical investigation. *J Theor Biol* 199:163–179
- Wagner H, Blickhan R (2003) Stabilizing function of antagonistic neuromusculoskeletal systems: an analytical investigation. *Biol Cybern* 199:163–179
- Wagner H, Siebert T, Ellerby DJ, Marsh RL, Blickhan R (2005) ISOFIT: a model-based method to measure muscle–tendon properties simultaneously. *Biomech Model Mechanobiol* 4:10–19
- Weihmann T, Blickhan R (2006) Legs operate different during steady locomotion and escape in a wandering spider. *J Biomech* 39(Suppl 1):361

- Wells JB (1965) Comparison of mechanical properties between slow and fast mammalian muscles. *J Physiol* 178:252–269
- Whitehead WF, Rempel JG (1959) A study of the musculature of the black widow spider, *Latrodectus mactans* (Fabr.). *Can J Zool* 37(6):831–870
- Woittiez RD, Huijing PA, Boom HB, Rozendal RH (1984) A three-dimensional muscle model: a quantified relation between form and function of skeletal muscles. *J Morphol* 182:95–113
- Woledge RC (1998) Possible effects of fatigue on muscle efficiency. *Acta Physiol Scand* 162:267–273
- Zebe E, Rathmayer W (1968) An electron microscopical study of spider muscles. *Z Zellforsch Mikrosk Anat* 92:377–387